

Comparative Study of Two-Stage and Segmented Thermoelectric Generators

Samson Shittu¹, Guiqiang Li^{1*}, Xudong Zhao¹, Xiaoli Ma¹

¹Centre for Sustainable Energy Technologies, University of Hull, HU6 7RX, UK

ABSTRACT

This paper presents a comparative study of two-stage, segmented and conventional thermoelectric generators. A detailed numerical study is performed using COMSOL Multiphysics and finite element method. The effects of thermoelectric leg height ratio, hot and cold side temperatures on the power output of the two-stage thermoelectric generator (TTEG), segmented thermoelectric generator (STEG) and conventional thermoelectric generator (TEG) are studied using three-dimensional numerical models. Results show that the TTEG and STEG provide an increased power output of 14.90% and 21.04% respectively compared to the skutterudite TEG at hot side temperature of 425 °C. Furthermore, it is found that the STEG is the best performing system studied and it provides an increased power output of 5.34% compared to that of the TTEG at 425 °C hot side temperature. In addition, results show that the power output of the TTEG and STEG increased respectively by 19.09% and 20.61% as the leg height ratio is increased from 1 to 4 for hot side temperature of 425 °C. Therefore, thermoelectric leg height ratio optimization is essential for performance enhancement.

Keywords: Thermoelectric generator, TTEG, STEG, Finite element method, Leg height

1. INTRODUCTION

A thermoelectric generator (TEG) is a solid state device that can convert heat into electricity directly using the Seebeck effect [1]. Advantages of the TEG include silent operation, high reliability, clean energy and long life span [2]. Recently, thermoelectric generator (TEG) has received increased attention due to its capacity to function as a waste heat recovery technology especially in applications which release a lot of waste heat such as

vehicles [3]. However, the low conversion efficiency of the TEG has hindered its wide spread application [4]. To enhance the efficiency of thermoelectric generators, a lot of researchers have paid attention to thermoelectric geometry optimization [5]. Geometries such as cascaded/two-stage TEG [6,7], segmented TEG [8,9] have been investigated and enhanced performance was obtained.

Thermoelectric materials are usually classified based on their operating temperature range and bismuth telluride (Bi_2Te_3) is used for low temperature operation ($< 200\text{ }^\circ\text{C}$) while skutterudite material is used for medium temperature operation ($< 500\text{ }^\circ\text{C}$) [10,11]. Therefore, two-stage thermoelectric generator (TTEG) and segmented thermoelectric generator (STEG) have received increased research attention because different materials can be combined such as low temperature and medium temperature materials to enhance the overall performance of the thermoelectric generator due to the materials operating at their most efficient temperature range [12].

This paper presents a comparative study of two-stage and segmented thermoelectric generators. The same thermoelectric materials are used in both the TTEG and STEG and leg height ratio optimization is performed. A three-dimensional numerical study is performed using COMSOL Multiphysics and finite element method. Furthermore, the TTEG and STEG are compared to a conventional TEG for different hot side and cold side temperatures.

2. MODEL DESCRIPTION

2.1 Physical model

The schematic diagrams of the three different thermoelectric generators considered in this study are

shown in Fig. 1. The two-stage thermoelectric generator (TTEG) shown in Fig. 1a consists of two different thermoelectric materials including bismuth telluride (n-type and p-type) material which is used for the lower stage while skutterudite material (n-type and p-type) is used for the upper stage. Both stages are connected in series electrically and in parallel thermally. Similarly, the segmented thermoelectric generator (STEG) shown in Fig. 1b contains the same materials as the TTEG while the conventional TEG shown in Fig. 1c has only one material. In the three systems, the same total leg height is used throughout the study (2.5 mm) to enable accurate comparison. However, for the TTEG and STEG, the height ratio (H_{us}/H_{ls}) is optimized. H_{us} is the leg height of the upper stage while H_{ls} is the leg height of the lower stage.

The geometrical parameters used in the thermoelectric generator is shown in Table 1. The TEG is connected to an external load resistance and impedance matching is done to obtain the maximum power output. The temperature dependent thermoelectric material properties used in this study are obtained from [13] while the remaining simulation parameters used in this study are obtained from [14]. Constant temperature boundary conditions are used on the hot and cold sides of the thermoelectric generator.

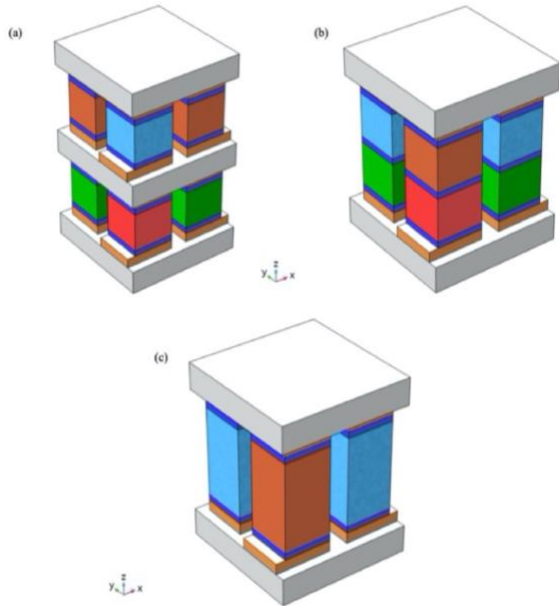


Fig. 1. Schematic diagram of (a) TTEG (b) STEG and (c) TEG.

Table 1. Geometrical parameters.

Parameter	Value
Ceramic	3.92 mm x 3.92 mm x 0.75 mm
Copper	1.4 mm x 1.4 mm x 0.3 mm
Solder	1.4 mm x 1.4 mm x 0.175 mm
Leg	1.4 mm x 1.4 mm x 2.5 mm

2.2 Governing equations

The electrical performance of the TEG is expressed as:

$$V_{OC} = \alpha \Delta T \quad (1)$$

where V_{OC} is the open circuit voltage, α is the Seebeck coefficient and ΔT is the TEG temperature difference.

$$V_L = V_{OC} - R_{in}I = R_L I \quad (2)$$

where V_L is the output load voltage, R_L is the external load resistance, R_{in} is the internal resistance of the TEG and I is the TEG current.

The output power of the TEG is given as,

$$P_{out} = V_L I = R_L I^2 \quad (3)$$

3. RESULTS AND DISCUSSION

3.1 Effect of thermoelectric leg height ratio

The variation of thermoelectric leg height ratio with the power output of a two-stage thermoelectric generator (TTEG) and segmented thermoelectric generator (STEG) is shown in Fig. 2. Under a fixed cold side temperature of 25 °C and varying hot side temperature of 275 – 425 °C, the thermoelectric leg height ratio is varied, and the power output obtained is shown in Fig. 2a. It can be seen that the optimum leg height ratio for both the TTEG and STEG is dependent on the hot side temperature used. Furthermore, it can be seen clearly that as the hot side temperature increases, the optimum leg height ratio increases. For hot side temperature of 275 °C and 325 °C, the optimum leg height ratio for the TTEG and STEG is 1.5 (i.e. $H_{us} = 1.5$ mm and $H_{ls} = 1$ mm). While the optimum leg height ratio for the TTEG and STEG is 4 (i.e. $H_{us} = 2$ mm and $H_{ls} = 0.5$ mm) when the hot side temperature is increased to 375 °C and 425 °C. The reason for this is that, skutterudite is the best performing thermoelectric material at medium temperature. Therefore, as the hot side temperature is increased beyond the operating temperature range of the bismuth telluride material, it is better to have a higher material proportion (i.e. leg height) of the skutterudite material with respect to the entire leg height. Furthermore, it can be seen from Fig. 2a that the power output of the TTEG and STEG increased respectively by 19.09% and 20.61% as the leg height ratio is increased from 1 to 4 for hot side temperature of 425 °C. This shows the importance of thermoelectric leg height ratio optimization.

Under a fixed hot side temperature of 425 °C and varying cold side temperature of 100 – 175 °C, the thermoelectric leg height ratio is varied, and the power output obtained is shown in Fig. 2b. It can be seen clearly

that for all the cold side temperatures considered, the optimum leg height ratio is 4. The reason for this is that, the cold side temperature considered is high and since a low temperature thermoelectric material (Bi_2Te_3) is used at the lower stage of the TTEG and STEG, it is better to have a higher proportion of skutterudite material to generate more power output. Basically, the high cold side temperature used means the lower stage thermoelectric material (Bi_2Te_3) has a reduced temperature difference to generate power output since it operates efficiently below 200°C . Therefore, it is obvious that if high cold side temperature is to be used, a high thermoelectric leg height ratio (i.e. 4) must be used to obtain enhanced performance.

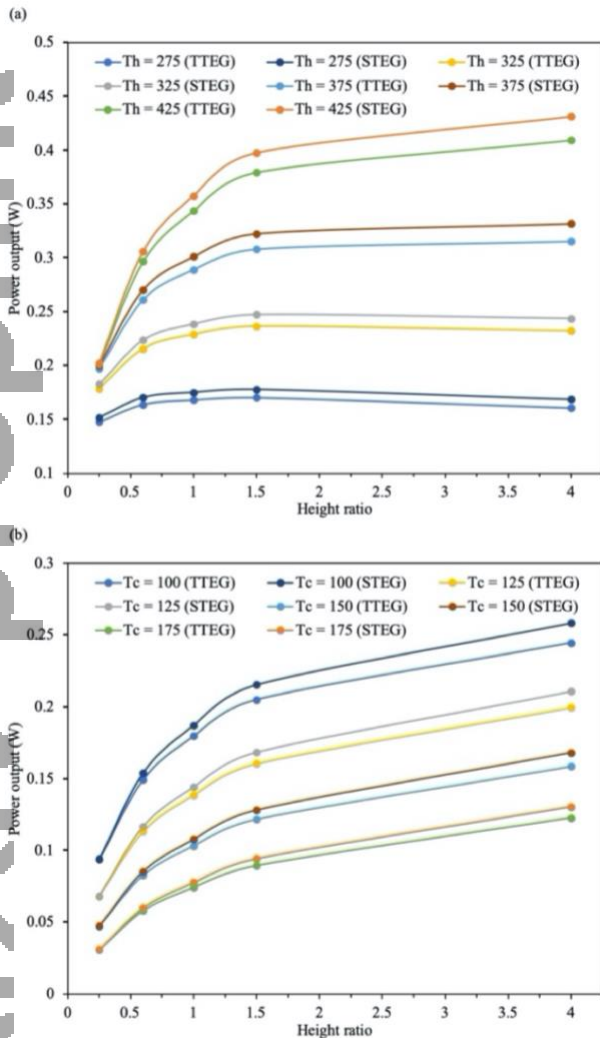


Fig. 2. Variation of height ratio with power output for different (a) hot side and (b) cold side temperatures.

3.2. Effect of hot and cold side temperatures

The power output of the TTEG, STEG, bismuth telluride TEG and skutterudite TEG for different hot and

cold side temperatures is shown in Fig. 3. Thermoelectric leg height ratio of 4 is used for both the TTEG and STEG. Under a fixed cold side temperature of 25°C and a varying hot side temperature, the power output of the different systems studied is shown in Fig. 3a. It can be seen that for the systems studied except the bismuth telluride TEG, the power output increases as the hot side temperature increases. This is expected as the increase in hot side temperature means an increase in temperature difference since the cold side temperature is fixed. Generally, increase in temperature difference leads to an increase in the power output of a thermoelectric generator. The reason for the power output decrease of the bismuth telluride TEG is that bismuth telluride material operates efficiently below 200°C . Therefore, as the hot side temperature is increased above its operating temperature, its power output decreases. Consequently, bismuth telluride TEG cannot be used for high temperature applications. Contrarily, skutterudite TEG, TTEG and STEG operate efficiently at high temperature and can be used for waste heat recovery in applications that release a lot of heat at high temperature. Furthermore, it can be seen that the TTEG and STEG both perform better than both conventional TEG especially at high temperature. In fact, the TTEG and STEG provide an increased power output of 14.90% and 21.04% respectively compared to the skutterudite TEG at hot side temperature of 425°C . Furthermore, it is obvious that the STEG is the best performing system studied and it provides an increased power output of 5.34% compared to that of the TTEG at 425°C hot side temperature. It is important to note that the STEG consumes a lower amount of material than the TTEG due to the absence of an additional ceramic layer and copper layer which is present in the TTEG.

Under a fixed hot side temperature of 425°C and a varying cold side temperature, the power output of the different systems studied is shown in Fig. 3b. It is obvious that the power output of all the systems decrease as the cold side temperature increases due to the decrease in temperature difference across the hot and cold sides of the thermoelectric generators. Therefore, effective cooling of thermoelectric generators is essential. However, it can be seen that the TTEG, STEG and skutterudite TEG are still able to generate some power even at high cold side temperatures. However, the bismuth telluride TEG requires a low cold side temperature to generate power since it is a low temperature material.

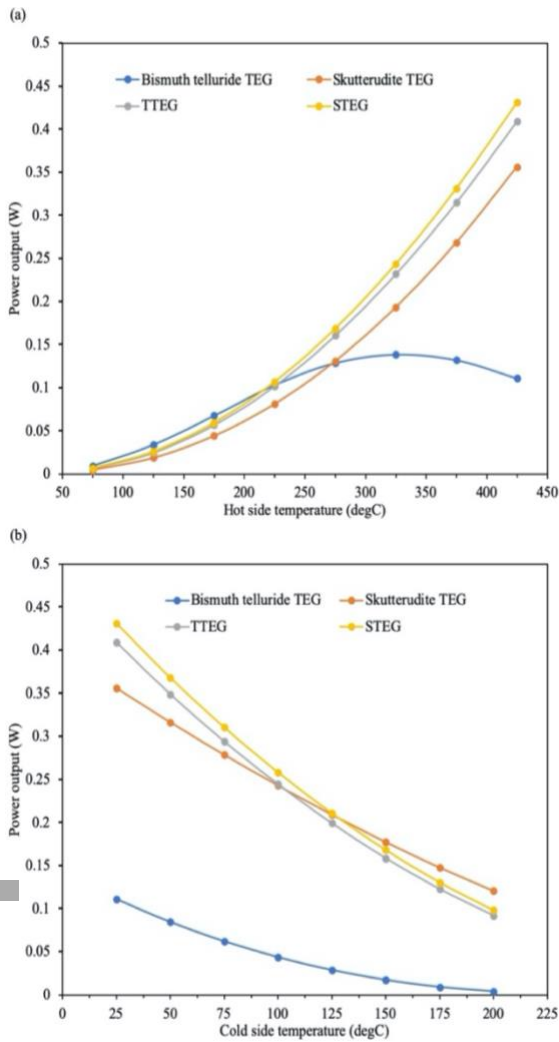


Fig. 3. Variation of power output with (a) hot side temperature and (b) cold side temperature.

3.3 Temperature and voltage distribution

The temperature and voltage distribution of the TTEG and STEG for thermoelectric leg height ratio of 4 is shown in Fig. 4 at a hot and cold side temperature of 425 °C and 25 °C respectively. As shown in Fig. 4a and Fig. 4c, the temperature in the TTEG and STEG respectively decrease from the top side to the bottom side due to fixed temperature boundary at the cold side. In addition, Fig. 4b and Fig. 4d show respectively the voltage distribution in the TTEG and STEG. It can be seen that the thermoelectric legs are connected electrically in series.

4. CONCLUSION

This paper presented a detailed numerical study of two-stage, segmented and conventional thermoelectric generators using COMSOL Multiphysics and finite element method. The effect of thermoelectric leg height

ratio on the power output of two-stage thermoelectric generator (TTEG) and segmented thermoelectric generator (STEG) was studied using three-dimensional numerical models. Furthermore, the effect of hot and cold side temperatures on the power output of the thermoelectric generator was presented and a comparison between the TTEG, STEG and conventional TEG was performed. It was found that the optimum thermoelectric leg height ratio for both the TTEG and STEG increases as the hot side temperature is increased. In addition, the power output of the TTEG and STEG increased respectively by 19.09% and 20.61% as the leg height ratio is increased from 1 to 4 for hot side temperature of 425 °C. This therefore shows the importance of thermoelectric leg height ratio optimization.

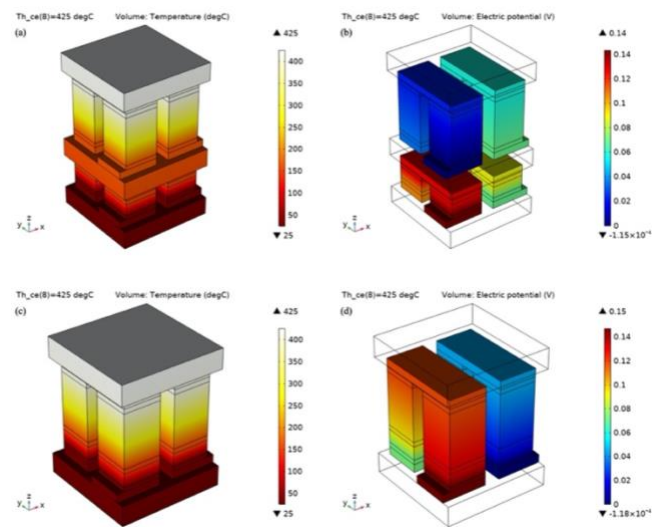


Fig. 4. TTEG (a) temperature distribution (b) voltage distribution; STEG (c) temperature distribution (d) voltage distribution.

REFERENCE

- [1] Shittu S, Li G, Zhao X, Ma X. Review of thermoelectric geometry and structure optimization for performance enhancement. *Appl Energy* 2020;268:115075. doi:10.1016/j.apenergy.2020.115075.
- [2] Shittu S, Li G, Zhao X, Ma X, Akhlaghi YG, Fan Y. Comprehensive study and optimization of concentrated photovoltaic-thermoelectric considering all contact resistances. *Energy Convers Manag* 2020;205:112422. doi:10.1016/j.enconman.2019.112422.
- [3] He W, Wang S, Zhang X, Li Y, Lu C. Optimization design method of thermoelectric generator based on exhaust gas parameters for recovery of engine waste heat. *Energy* 2015;91:1–9.

- doi:10.1016/j.energy.2015.08.022.
- [4] Shittu S, Li G, Zhao X, Zhou J, Ma X. Experimental study and exergy analysis of photovoltaic-thermoelectric with flat plate micro-channel heat pipe. *Energy Convers Manag* 2020;207:112515. doi:10.1016/j.enconman.2020.112515.
- [5] Shittu S, Li G, Tang X, Zhao X, Ma X, Badiei A. Analysis of thermoelectric geometry in a concentrated photovoltaic-thermoelectric under varying weather conditions. *Energy* 2020;202:117742. doi:10.1016/j.energy.2020.117742.
- [6] Sun H, Ge Y, Liu W, Liu Z. Geometric optimization of two-stage thermoelectric generator using genetic algorithms and thermodynamic analysis. *Energy* 2019;171:37–48. doi:10.1016/j.energy.2019.01.003.
- [7] Liu Z, Zhu S, Ge Y, Shan F, Zeng L, Liu W. Geometry optimization of two-stage thermoelectric generators using simplified conjugate-gradient method. *Appl Energy* 2017;190:540–52. doi:10.1016/j.apenergy.2017.01.002.
- [8] Shittu S, Li G, Zhao X, Ma X, Akhlaghi YG, Ayodele E. Optimized high performance thermoelectric generator with combined segmented and asymmetrical legs under pulsed heat input power. *J Power Sources* 2019;428:53–66. doi:10.1016/j.jpowsour.2019.04.099.
- [9] Shittu S, Li G, Zhao X, Ma X, Akhlaghi YG, Ayodele E. High performance and thermal stress analysis of a segmented annular thermoelectric generator. *Energy Convers Manag* 2019;184:180–93. doi:10.1016/j.enconman.2019.01.064.
- [10] Shittu S, Li G, Akhlaghi YG, Ma X, Zhao X, Ayodele E. Advancements in thermoelectric generators for enhanced hybrid photovoltaic system performance. *Renew Sustain Energy Rev* 2019;109:24–54. doi:10.1016/j.rser.2019.04.023.
- [11] Shittu S, Li G, Xuan Q, Xiao X, Zhao X, Ma X. Transient and non-uniform heat flux effect on solar thermoelectric generator with phase change material. *Appl Therm Eng* 2020;173:115206. doi:10.1016/j.applthermaleng.2020.115206.
- [12] Snyder GJ. Application of the compatibility factor to the design of segmented and cascaded thermoelectric generators. *Appl Phys Lett* 2004;84:2436–8. doi:10.1063/1.1689396.
- [13] Fan S, Gao Y. Numerical analysis on the segmented annular thermoelectric generator for waste heat recovery. *Energy* 2019;183:35–47. doi:10.1016/j.energy.2019.06.103.
- [14] Shittu S, Li G, Xuan Q, Zhao X, Ma X, Cui Y. Electrical and mechanical analysis of a segmented solar thermoelectric generator under non-uniform heat flux. *Energy* 2020;199:117433. doi:10.1016/j.energy.2020.117433.